

Quantum squeezing by a parametric resonance in a SQUID

T. Ojanen^{1*} and J. Salo²

¹*Low Temperature Laboratory, Helsinki University of Technology,
P. O. Box 2200, FIN-02015 HUT, Finland* and

²*Laboratory of Physics, Helsinki University of Technology, P. O. Box 4100, FIN-02015 HUT, Finland*

(Dated: October 21, 2018)

We study rotating squeezed quantum states created by a parametric resonance in an open harmonic system. As a specific realization of the phenomenon we study a mesoscopic SQUID loop where the state preparation procedure is simple in principle and feasible with currently available experimental methods. By solving dynamics and calculating spectral properties we show that quantum fluctuations of SQUID observables can be reduced below their groundstate value. The measurement is introduced by coupling the SQUID to a transmission line carrying the radiation to a secondary measurement device. Besides the theoretical interest, our studies are motivated by an opportunity for a practical quantum noise engineering.

I. INTRODUCTION

At the heart of the quantum theory lies the fundamental principle of describing physically observable quantities as Hermitian operators acting on Hilbert space of quantum states. Generally these operators do not commute, a trait giving rise to the fundamental uncertainty principle first formulated by Heisenberg. The uncertainty principle characterizes the statistical spread of the distributions corresponding to two different observables. If the operators representing the observables do not commute, the statistical variations of their observed distributions, frequently called uncertainties, cannot generally be arbitrarily small in a given state. However, the statistical variation of a single observable is not limited in any way by the uncertainty principle. For two given non-commuting observables, a state in which the lower limit of the uncertainty principle is reached is called a minimum uncertainty state. Decreasing the uncertainty with respect to one observable results in the increase of the uncertainty of the other. The transfer of uncertainty from one observable to another with respect to the minimum uncertainty values is referred to as squeezing. The squeezing of quantum fluctuations was first studied and experimentally verified in quantum optics, where the components of quantized electric field served as the squeezed observables.^{1,2} Since then the phenomenon has been observed in superconducting circuits,^{3,4} and more recently, there has been a promising efforts to realize the squeezing in nanomechanical structures.⁵

Due to the technological advances, the development in mesoscopic physics has been rapid in last decades, and many interesting quantum phenomena have been experimentally verified for the first time. Also a number of new and important measuring devices, necessary to observe elementary quantum phenomena, have been invented. In this paper we study the phenomena of the quantum squeezing in a mesoscopic Superconducting QUantum Interference Device (SQUID), with emphasis on the creation and consequences of the squeezing. However, the squeezing is an example of a manipulation of quantum fluctuations which could have direct applications in a

practical quantum measurement.

Experimentally the squeezing of the quantum fluctuations has been demonstrated in microwave frequencies by constructing a Josephson parametric amplifier,⁴ with a 40% reduction of the vacuum noise. Theoretically the squeezing has been studied in a similar SQUID ring we consider here.⁶ The squeezing mechanism we study is different from one studied in Ref. 6 which was based on a rapid decrease of an external magnetic flux to switch on the Josephson coupling. We consider a parametric instability in a harmonic regime,⁷ a well-known procedure to create the squeezing and applicable in various different systems.⁸ It can be realized with an elementary flux control in an rf SQUID. In the limit of a negligible dissipation the magnitude of the squeezing is exponential in short times and, it rotates between the charge and the magnetic flux of the SQUID. A strong dissipation compensates the resonant driving and leads to a rotating quasistationary state where uncertainties periodically go below their groundstate values. We calculate the noise spectrum of periodic squeezed states and discuss the measurement problem by analyzing a setup where the SQUID is coupled to a transmission line.

II. SQUEEZING BY PARAMETRIC RESONANCE

The parametric resonance is a well-known physical phenomena in a classical harmonic oscillator (HA).⁹ A periodic time-dependent perturbation can lead to large effects, which are most significant when the period of the perturbation is twice the resonance frequency. Driven in resonance, the energy of the system grows exponentially in time. This is true for a quantum HA also.⁸ In addition, starting the resonant driving from the groundstate of HA it results in a rapid squeezing of the uncertainties of the conjugate observables of HA. Consider the Hamiltonian

$$H = \frac{p^2}{2m} + \frac{m\omega^2(t)}{2}x^2, \quad (1)$$

where p and x are the canonical variables $[x, p] = i\hbar$, m is the mass constant and the time-dependent dependent perturbation is included in $\omega^2(t) = \omega_0^2 + A \cos 2\omega_0 t$. Furthermore, let us assume that the time-dependent part can be treated as a perturbation, $|A| \ll \omega_0^2$. The ground-state of the free Hamiltonian ($A = 0$) in the position representation is $\psi_0(x) = \pi^{-1/4} \alpha^{1/4} \exp(-\alpha x^2/2)$, where $\alpha = 1/l_0^2 = m\omega_0/\hbar$ is an inverse square of the characteristic zero point length scale. An approximate solution to the Schrödinger equation corresponding to the Hamiltonian of Eq. (1) and the initial condition $\psi(x, t = 0) = \psi_0(x)$ can be obtained analytically in the Gaussian form

$$\psi(x, t) = \left(\frac{\text{Re } \alpha(t)}{\pi} \right)^{1/4} \exp(-\alpha(t) x^2/2), \quad (2)$$

where

$$\alpha(t) = \frac{i}{l_0^2} \frac{(1 - ie^{2\xi}) \sin(\omega_0 t) + (1 + ie^{2\xi}) \cos(\omega_0 t)}{-(1 + ie^{2\xi}) \sin(\omega_0 t) + (1 - ie^{2\xi}) \cos(\omega_0 t)} \quad (3)$$

with $\xi = At/4\omega_0$. Physically Eq. (2) describes a wave packet centered at $x = 0$, but whose width oscillates in time with an exponentially growing amplitude. When the statistical spread in the real space is the widest, the corresponding spread in the momentum space is the smallest. Defining the dimensionless quantities $x' = x/l_0$ and $p' = p l_0/\hbar$ we discover that in the state (2) we have $\Delta x' \Delta p' = \langle x'^2 \rangle^{1/2} \langle p'^2 \rangle^{1/2} = |\langle [x', p'] \rangle|/2 = 1/2$ and the state remains minimum uncertainty state at all times. The individual deviations may be written as

$$\Delta x' = \frac{\beta}{\sqrt{2}} \quad \Delta p' = \frac{\beta^{-1}}{\sqrt{2}}, \quad (4)$$

where $\beta = (\text{Re } \alpha(t))^{-1/2}/l_0$. From Eq. (3) we obtain

$$\text{Re } \alpha(t) = \frac{1}{l_0^2} (\sinh^2 \xi + \cosh^2 \xi - 2 \sin(2\omega_0 t) \sinh \xi \cosh \xi)^{-1} \quad (5)$$

The maximum uncertainty oscillates with a frequency $2\omega_0$ between the position and momentum. At the times corresponding to $\sin(2\omega_0 t) = \pm 1$ the squeezing is given by $\beta = e^{\mp \xi}$. The solution (2) is very accurate as long as the condition $A \ll \omega_0^2$ holds. If $A \lesssim 0.1\omega_0^2$ the analytical solution agrees excellently with the exact solution up to the squeezing factor 5, see Fig. 1. After that the lower value does not decrease further as in the analytical solution even though the general agreement is accurate.

The above example illustrates the mechanism behind the squeezing scheme we will now apply to a flux-controlled rf SQUID loop described in Fig. 2. The Hamiltonian for the system can be written as

$$H = \frac{Q^2}{2C} + \frac{\phi^2}{2L_S} + E_J \cos(\Phi(t) 2e/\hbar) \cos(\phi 2e/\hbar), \quad (6)$$

where C is the capacitance of the junctions, L_S is the self-inductance of the loop and $\Phi(t)$ is the flux bias externally

applied through the smaller loop.¹⁰ The quantities Q and ϕ are the canonical variables corresponding to the charge in the capacitor and the magnetic flux in the loop and satisfy the commutation relation $[\phi, Q] = i\hbar$. Thus the magnetic flux ϕ plays the role of the position coordinate and the charge Q corresponds to the momentum in the standard one-particle quantum mechanics. The flux value corresponding to the oscillator length l_0 of the harmonic part of (6) is $\phi_0 = \sqrt{\hbar Z_0}$, where $Z_0 = \sqrt{L_S/C}$.

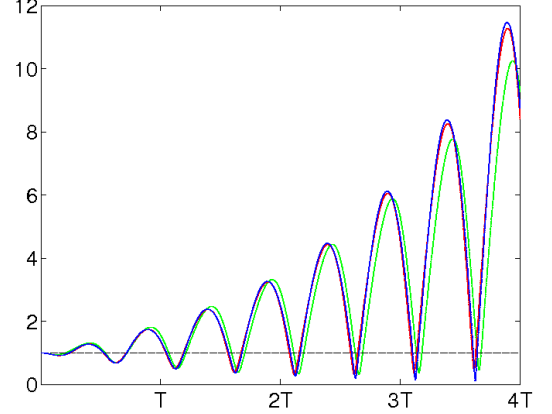


FIG. 1: (Color online) Uncertainty of the magnetic flux $\sqrt{2\Delta\phi}$ in time. The parametric driving with a strength $B = 0.1\omega_0^2$ makes the uncertainty to oscillate with the frequency $2\omega_0$ below and above the groundstate value marked by the black dashed line. The blue line corresponds to the analytical solution, the red line to the exact numerical solution and the green line to the exact solution with the AC flux modulation (9).

We treat the Josephson term as a perturbation and therefore consider the parameter range $L_S \ll L_J$, where we have defined the Josephson inductance as $L_J = \hbar^2/4e^2 E_J$. If the quadratic potential is strong, the flux particle is restricted to the linear regime of the SQUID and the term $\cos(\phi 2e/\hbar)$ may be expanded to the second order. Supposing that the condition for the validity of the approximation $\phi_0 < \Phi_0 = h/2e$ is satisfied, the Hamiltonian (6) takes the form

$$H \approx \frac{Q^2}{2C} + \frac{\phi^2}{2L_S} - \frac{\phi^2}{2L_J} \cos(\Phi(t) 2e/\hbar) = \frac{Q^2}{2C} + \frac{C\omega^2(t)}{2} \phi^2, \quad (7)$$

where

$$\omega^2(t) = \omega_0^2 \left(1 - \frac{L_S}{L_J} \cos(\Phi(t) 2e/\hbar) \right) \quad (8)$$

with $\omega_0^2 = (L_S C)^{-1}$. In the cosine expansion the small term constant in ϕ has been dropped from Eq. (7). Now we have established a connection between Eqs. (1) and (7) provided that the external magnetic flux is modulated according to $\Phi(t) = \hbar\omega_0 t/e$. This could be achieved

by increasing the magnetic field linearly inside the control loop. The temporal evolution of the SQUID starting from the groundstate is readily solved by identifying $A \rightarrow \omega_0^2(L_S/L_J)$ and $l_0 \rightarrow \phi_0$ and applying Eqs. (2) and (5). The dimensionless operators $\phi' = \phi/\phi_0$ and $Q' = Q\phi_0/\hbar$ satisfy the minimum uncertainty condition $\Delta\phi'\Delta Q' = 1/2$ and the individual deviations behave as those in Eq. (4).

The linearly increasing magnetic flux is inconvenient practically since the magnetic field should be restricted to the control loop and it is difficult to isolate at high field values. In addition, the AC fields are obtained and manipulated more easily. From the approximate equivalence $\cos(2x) \approx \cos(3\sin(x))$ can be inferred that if the magnetic flux is modulated with an AC field according to

$$\Phi(t) = (3/2\pi)\Phi_0 \sin(\omega_0 t), \quad (9)$$

then $\cos(\Phi(t)2e/\hbar) \approx \cos(2\omega_0 t)$. Hence the magnetic flux should be modulated at the resonance frequency such a way that its amplitude is roughly a half of the flux quantum.

For later purposes it is convenient to introduce the second-quantized creation and annihilation operators in the photon number Fock space. The SQUID observables may be written as

$$\phi = \sqrt{\frac{\hbar Z_0}{2}}(a + a^\dagger), \quad Q = i\sqrt{\frac{\hbar}{2Z_0}}(a^\dagger - a). \quad (10)$$

Operators a, a^\dagger satisfy the usual bosonic commutation relations. In this language the Hamiltonian Eq. (7) is transformed to

$$H = \hbar\omega_0(a^\dagger a + \frac{1}{2}) + B \cos(2\omega_0 t)(a + a^\dagger)^2, \quad (11)$$

where $B = \hbar\omega_0 L/4L_J$. In the case where expectation values of ϕ and Q vanish, as above, the root mean square deviations may be written as

$$\begin{aligned} \Delta\phi' &= \frac{1}{\sqrt{2}}(\langle a^2 \rangle + \langle a^{\dagger 2} \rangle + \langle aa^\dagger \rangle + \langle a^\dagger a \rangle)^{1/2} \\ \Delta Q' &= \frac{1}{\sqrt{2}}(-\langle a^2 \rangle - \langle a^{\dagger 2} \rangle + \langle aa^\dagger \rangle + \langle a^\dagger a \rangle)^{1/2}. \end{aligned} \quad (12)$$

III. COUPLING THE SQUID TO A TRANSMISSION LINE

In this section we introduce a measuring scheme in which the SQUID is coupled to a transmission line (TL) which serves as a wave guide carrying the radiation away from the system. It also plays a role of a generic measurement device which causes a Markovian back-action to the measured system. In addition, the TL provides a practical theoretical model for studying the environmental effects to the squeezing.

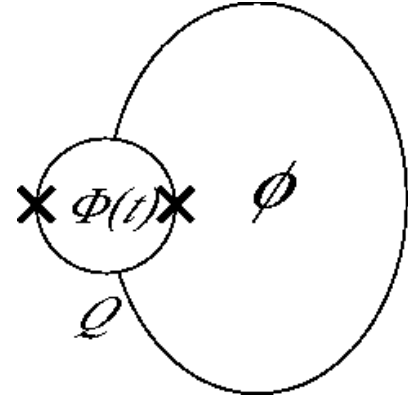


FIG. 2: Schematic representation of the SQUID loop. The crosses represent Josephson junctions and the physical quantities ϕ and Q correspond to the magnetic flux through the main loop and the charge at the junctions. The flux $\Phi(t)$ through the smaller loop is controlled by an external magnetic field.

The study of a non-classical radiation requires a quantum-mechanical treatment of the SQUID and the TL. Quantum mechanics of a TL is essentially similar with a one-dimensional quantized electromagnetic field and it has been discussed in Ref. 11. Consider the sys-

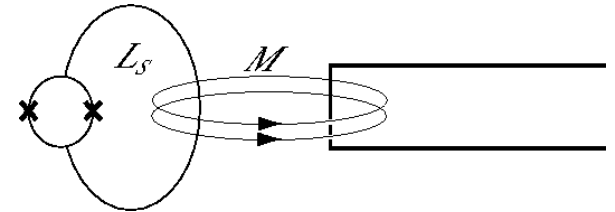


FIG. 3: Transmission line inductively coupled to the SQUID.

tem in Fig. 3 where the SQUID is magnetically coupled to a TL. The magnetic flux of the nearby SQUID penetrates into the TL. The inductance and capacitance per unit length in the TL are l and c and the wave velocity is given by $v = 1/\sqrt{lc}$.

The Lagrangian for the line can be written as

$$\mathcal{L} = \int_0^L dx \left(\frac{l}{2} j^2 - \frac{c}{2} q^2 \right), \quad (13)$$

where $j(x, t)$ and $q(x, t)$ are the local current and charge densities. Following Ref. 11 we introduce a new variable

$$\theta(x, t) \equiv \int_0^L dx' q(x', t), \quad (14)$$

which, together with the continuity equation, allows one to write the Lagrangian

$$\mathcal{L} = \int_0^L dx \left(\frac{l}{2} \dot{\theta}^2 - \frac{c}{2} (\partial_x \theta)^2 \right). \quad (15)$$

From the total charge neutrality that it follows that $\theta(0, t) = \theta(L, t) = 0$, so θ can be expanded by the eigenmodes

$$\theta(x, t) = \sqrt{\frac{2}{L}} \sum_k A_k(t) \sin(\beta_k x), \quad (16)$$

where $b_k = k\pi/L$ and the Lagrangian takes the form

$$\mathcal{L} = \sum_k \left(\frac{l}{2} \dot{A}_k^2 - \frac{\beta_k^2}{2c} A_k^2 \right). \quad (17)$$

The quantization of the quadratic Lagrangian (17) is well known. The Hamiltonian can be written as

$$H^{\text{TL}} = \sum_k \left(\frac{l}{2} \Pi_k^2 + \frac{\beta_k^2}{2c} A_k^2 \right), \quad (18)$$

where $[A_k, \Pi_k] = i\hbar$. This can be further written with the help of bosonic creation and annihilation operators c_k and c_k^\dagger as

$$\begin{aligned} A_k &= \sqrt{\frac{\hbar\omega_k c}{2}} \frac{1}{\beta_k} (c_k(t) + c_k^\dagger(t)) \\ \Pi_k &= -i\sqrt{\frac{\hbar\omega_k l}{2}} (c_k(t) - c_k^\dagger(t)), \end{aligned} \quad (19)$$

and the Hamiltonian (18) becomes

$$H^{\text{TL}} = \sum_m \hbar\omega_k (c_m^\dagger c_m + 1/2). \quad (20)$$

The eigenfrequencies are defined as $\omega_k = \beta_k v$. The voltage and current operators in the TL can be derived from θ as $V(x, t) = (1/c)\partial_x \theta(x, t)$ and $I(x, t) = \dot{\theta}(x, t)$. The magnetic interaction between the SQUID and the TL couples the operators $I_S = \phi/L_S$ and $I(x, t)$, where I_S and L_S are the current and the inductance of the SQUID loop. Supposing that the SQUID couples to each mode approximately as strongly, the interaction may be written as

$$H_{\text{int}} = M \frac{\phi}{L_S} \sum_k i \sqrt{\frac{\hbar\omega_k}{Ll}} (-c_k + c_k^\dagger), \quad (21)$$

where M is the mutual inductance between the SQUID and the field mode.

Now we could proceed to two directions. On one hand we could study the SQUID Hamiltonian by trying to eliminate the transmission line variables (and other possible environment modes). On the other hand we are interested in the TL output radiation to measure the SQUID. The first problem leads to a master equation description of the SQUID and it will be studied in the next section. The latter problem will be pursued here.

From the Heisenberg equation of motion for the operators c_k we obtain

$$\partial_t c_k = -i\omega_k c_k + \frac{M}{L_S} \sqrt{\frac{\omega_k}{\hbar Ll}} \phi \quad (22)$$

which can be solved as

$$\begin{aligned} c_k(t) &= c_k(0) e^{-i\omega_k t} + \\ &\quad \frac{M}{L_S} \sqrt{\frac{\omega_k}{\hbar Ll}} e^{-i\omega_k t} \int_0^t \phi(t') e^{i\omega_k t'} dt', \end{aligned} \quad (23)$$

where $\phi(t)$ is the flux operator of the SQUID. From this expression one can see that the TL problem can be solved as soon as the the solution to the associated SQUID problem is known. The flux $\phi(t)$ is the only SQUID variable entering to the expression (23) and can be solved independently provided that the TL variables can be successfully eliminated from the SQUID dynamics. Substituting the expression (23) into the formula for the voltage of the TL

$$V(x, t) = \sum_k \sqrt{\frac{\hbar\omega_k}{Lc}} \cos \frac{k\pi x}{L} [c_k(t) + c_k^\dagger(t)], \quad (24)$$

we get

$$V(x, t) = V_0(x, t) + \frac{M\omega_0}{\pi L_S} \phi(t - x/v), \quad (25)$$

where $V_0(x, t)$ is the voltage operator of the free TL and the second term is proportional to the retarded SQUID field. Deriving Eq. (25) we have assumed that the level separation in the TL is much smaller than ω_0 , so the TL will act as a waveguide and not as a resonator. The current of the TL has a similar expression.

IV. THE ROLE OF THE DISSIPATION AND DECOHERENCE

A. Dissipative state evolution of the SQUID

So far we have treated the SQUID as an ideal system without any dissipation and decoherence effects. Real mesoscopic systems are much larger than the systems usually studied in atomic and molecular physics and generally need to be considered as open quantum systems. Also an important source of decoherence is the quantum measurement process in which the system is necessarily coupled to the external world. A state of an open quantum system can no longer be represented by simply a state vector making it necessary to introduce the density operator. The dissipation, energy absorption and suppression of quantum coherence effects can be naturally discussed within the density operator approach.

Assuming that the level separation in the SQUID loop is significantly higher than the temperature of the environment $\hbar\omega_0 > k_B T$, the dominating environmental effect is the spontaneous emission. The dynamics of the density operator after the Born-Markov elimination of the electromagnetic field modes can be described by a Lindblad master equation¹² of the form

$$\partial_t \rho = -\frac{i}{\hbar} [H, \rho] + \kappa (2a\rho a^\dagger - a^\dagger a \rho - \rho a^\dagger a), \quad (26)$$

where the first term is responsible for the Hamiltonian evolution by the operator (11) and the second term describes the spontaneous emission into the TL, which is assumed not to bring any signal back to the SQUID. The coefficient κ is related to the quality factor of the circuit by $\kappa = \omega_0/Q$. In the case of a free SQUID the Q -factor can be as high as $10^3 - 10^4$. The coupling to the TL should decrease Q significantly to guarantee an efficient measurement of the SQUID. The value of κ can be estimated then as $\kappa \approx (M/L_S)^2 Z_0/Z_{\text{TL}}$, where $Z_{\text{TL}} = \sqrt{l/c}$. The disadvantage of decreased Q is the increased decoherence which is hostile to the squeezing process.

B. Expectation values

Starting from Eq. (26) it is possible to derive the equations of motion for the expectation values of the creation and annihilation operators,

$$\begin{aligned} \partial_t \langle a \rangle &= (-i\omega_0 - \kappa - 2iB \cos(2\omega_0 t)) \langle a \rangle \\ &\quad - 2iB \cos(2\omega_0 t) \langle a^\dagger \rangle, \\ \partial_t \langle a^\dagger \rangle &= (+i\omega_0 - \kappa + 2iB \cos(2\omega_0 t)) \langle a^\dagger \rangle \\ &\quad + 2iB \cos(2\omega_0 t) \langle a \rangle, \end{aligned} \quad (27)$$

as well as for those of the quadratic operators

$$\begin{aligned} \partial_t \langle a^\dagger a \rangle &= 2iB \cos(2\omega_0 t) (\langle a^2 \rangle - \langle a^{\dagger 2} \rangle) - 2\kappa \langle a^\dagger a \rangle \\ \partial_t \langle a^2 \rangle &= -2i\omega_0 \langle a^2 \rangle - iB \cos(2\omega_0 t) \times \\ &\quad (4\langle a^2 \rangle + 4\langle a^\dagger a \rangle + 2) - 2\kappa \langle a^2 \rangle \\ \partial_t \langle a^{\dagger 2} \rangle &= 2i\omega_0 \langle a^{\dagger 2} \rangle + iB \cos(2\omega_0 t) \times \\ &\quad (4\langle a^{\dagger 2} \rangle + 4\langle a^\dagger a \rangle + 2) - 2\kappa \langle a^{\dagger 2} \rangle. \end{aligned} \quad (28)$$

These two present a closed set of equations. The missing combination $\langle a a^\dagger \rangle$ can be deduced from the commutation relation $[a, a^\dagger] = 1$. By solving the above equation system we obtain the uncertainties (12). The nature of solutions to the system (28) depends on the relative magnitudes of κ and B . If $\kappa > B$, the dissipation will eventually compensate the resonant driving and the solutions are periodic and bounded. Otherwise the expectation values grow increasingly in time. This, however, does not imply increasing squeezing of quantities (12). In the presence of dissipation the lowest value of the fluctuations has a finite lower limit.

By expanding the expectation values in Eq. (28) to a Fourier series and truncating them to the fourth order, we found an accurate analytical form for the periodic solution. In the limit $\kappa \rightarrow B + 0$, the lower limit of the periodic squeezing is about 0.75 times the vacuum value of $\Delta\phi'$ and $\Delta Q'$, see Fig. 5.

The nature of squeezed states in the presence of the dissipation is somewhat different from the pure squeezed states. The pure squeezed states are linear combinations of the even photon number states. The dissipation

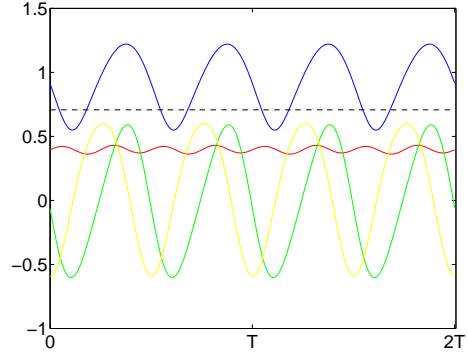


FIG. 4: (Color online) Two periods of the stationary solution $\kappa = 1.5B$. The blue curve is $\Delta\phi'$ and the red curve $\langle a^\dagger a \rangle$. The yellow and the green curves correspond to $\text{Re} \langle a^2 \rangle$ and $\text{Im} \langle a^2 \rangle$ respectively. The black horizontal dashed line marks the groundstate value of $\Delta\phi'$.

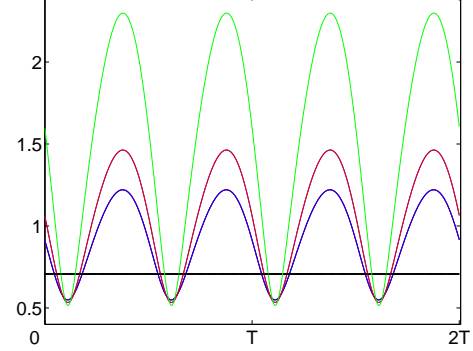


FIG. 5: (Color online) Uncertainty $\Delta\phi'$ of the bounded periodic solutions $\kappa = 1.5B$ (blue), $\kappa = 1.3B$ (red) and $\kappa = 1.1B$ (green). The black horizontal dashed line marks the groundstate value of $\Delta\phi'$. The minimum of the squeezing in the periodic solutions approaches to lower bound of about 0.75 times the groundstate value.

changes the spectral content so that the odd number photon states are also occupied. The resulting state is no longer a minimum certainty state, see Fig. 6.

C. Two-time correlation functions

In order to find the spectral properties of the signal radiated into the TL, we also need to evaluate two-time correlation functions, such as $\langle a^\dagger(t_2)a(t_1) \rangle$. According to the quantum regression formula¹², the function pair $\langle A(t)a(t') \rangle$ and $\langle A(t)a^\dagger(t') \rangle$ obey the same differential equations than $\langle a(t') \rangle$ and $\langle a^\dagger(t') \rangle$ for arbitrary operator $A(t)$. Choosing $A(t)$ to $a(t)$ we get

$$\begin{aligned} \partial_{t'} \langle a(t)a(t') \rangle &= (-i\omega_0 - \kappa - 2iB \cos(2\omega_0 t')) \langle a(t)a(t') \rangle \\ &\quad - 2iB \cos(2\omega_0 t') \langle a(t)a^\dagger(t') \rangle, \\ \partial_{t'} \langle a(t)a^\dagger(t') \rangle &= (+i\omega_0 - \kappa + 2iB \cos(2\omega_0 t')) \langle a^\dagger(t)a(t') \rangle \\ &\quad + 2iB \cos(2\omega_0 t') \langle a(t)a(t') \rangle \end{aligned} \quad (29)$$

for $t' > t$. A similar pair of equations hold for $\langle a^\dagger(t)a(t') \rangle$ and $\langle a^\dagger(t)a^\dagger(t') \rangle$. Solving Eqs. (29) and the correspond-

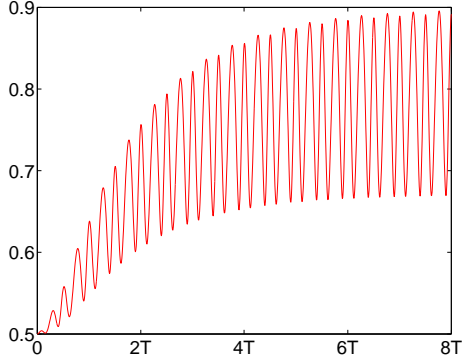


FIG. 6: (Color online) Evolution of the uncertainty product $\Delta\phi'\Delta Q'$ from the groundstate to the periodic steady state $\kappa = 1.5B$. After reaching the steady state, the uncertainty product oscillates with a frequency $4\omega_0$ about the constant value.

ing equations to the other pair, we can deduce an arbitrary second-order correlator in the whole time domain by using symmetries of the correlators.

D. Wigner function of the squeezed state

An intuitive way to perceive the squeezing phenomena is to plot the Wigner function

$$\rho_W(x', p') = (2\pi)^{-1} \int_{-\infty}^{\infty} \langle x' - \frac{1}{2}y | \rho | x' + \frac{1}{2}y \rangle e^{ip'y} dy. \quad (30)$$

The Wigner function is one of the quantum-mechanical analogues to the phase space probability distribution. Even though it is not a genuine 2-dimensional probability distribution, it has the property of giving the one-dimensional marginal distributions in arbitrary directions in the phase space (x', p') and can therefore be used directly to illustrate the uncertainties of observables. The groundstate of the SQUID has a circular symmetry which is distorted to an ellipse by squeezing, see Fig. 7. For ideal squeezed states the principal axes of elliptical contour lines are inversely proportional reflecting the minimum uncertainty property. The primary effect of the dissipation is to broaden the shorter axis resulting in an excess uncertainty.

V. SPECTRUM OF PARAMETRIC RESONANCE AND SQUEEZING

Based on Eq. (25) the spectral properties of $V(X, t)$ are directly related to spectral properties of ϕ and the free TL spectrum. Here we evaluate ϕ -noise and, at the end of the section, discuss parameters relevant to the TL output noise.

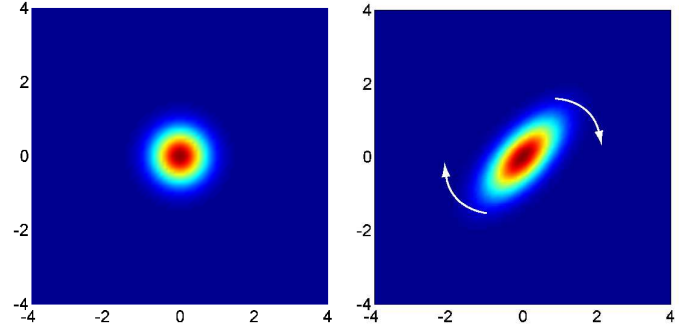


FIG. 7: (Color online) Wigner function of the groundstate (left) and the periodic squeezed state $\kappa = 1.5B$ (right) in the (ϕ', Q') -plane. The squeezed state rotates clockwise as indicated by the arrows. The ellipse makes 2π rotation in time $T = 2\pi/\omega_0$.

A. Time-averaged spectrum

The spectrum contains information about radiation emitted from the studied system. In Ref. 11 an excitation of a two-level system with an energy splitting $\Omega = \Delta E$ is considered as a spectrum analyzer. The probability to detect the analyzer system in either of its states is proportional to

$$\int_0^t \int_0^t \langle A(t_1)A(t_2) \rangle e^{-i\omega(t_2-t_1)} dt_1 dt_2 \quad (31)$$

at $\omega = \pm\Omega$, where A is an operator of the studied noise source which couples to the analyzer two-level system. Supposing that the system is in a steady state and the correlation time is short, the expression (31) reduces to $tS_A(\omega)$, where

$$S_A(\omega) = \int_{-\infty}^{\infty} \langle A(\tau)A(0) \rangle e^{i\omega\tau} d\tau. \quad (32)$$

The expression (32) is positive definite and determines the transition rates of the analyzer system. In the strong damping regime the SQUID radiation is periodic and the steady-state expression (32) is not appropriate as such. Rather, the detector rates are proportional to the time-averaged noise power

$$S_A(\omega) = \int_{-\infty}^{\infty} \frac{1}{T} \int_0^T \langle A(\tau+t')A(t') \rangle e^{i\omega\tau} dt' d\tau, \quad (33)$$

where T is the period of the motion. The expression (33) generalizes (32) in the sense that so defined spectrum is positive definite and gives excitation probabilities of the analyzer system in the long-time limit $t \gg T = 2\pi/\omega_0$. Since the SQUID couples to the TL with the operator $\phi' = (a + a^\dagger)/\sqrt{2}$, the ϕ' -spectrum is relevant in the TL radiation.

From the time-averaged observables it is difficult to detect the squeezing directly. This can be understood by considering the Wigner function. The fast rotation of the elliptic figure in Fig. 7 averages out to a circular shape where no squeezing is present. The ϕ -spectrum (33) of the SQUID in parametric resonance resembles to a spectrum of a dissipative harmonic oscillator at finite temperature, see Fig. 8. The spectrum displays peaks at frequencies $-\omega_0$ and ω_0 corresponding to emission and absorption processes. A study of a fine structure also reveals weak resonance peaks at frequencies $-3\omega_0$ and $3\omega_0$. These are the higher harmonics produced by the parametric driving process. In principle there is also resonance at higher odd multiples of ω but they are extremely weak compared to $-\omega_0$ and ω_0 peaks. The distance between the peaks is 2ω which characterizes the periodicity of the rotating squeezing.

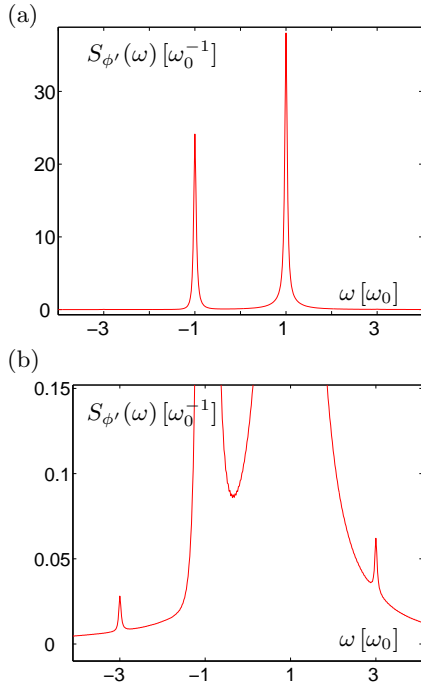


FIG. 8: (Color online) (a) Time-averaged noise spectrum $S_{\phi'}(\omega)$ of the periodic squeezed state $\kappa = 0.15\omega_0 = 1.25B$. The Spectrum has resonances at frequencies $\pm\omega_0$. (b) The fine structure of spectrum (a) reveals the weak resonance peaks at $\pm 3\omega_0$.

B. Spectrum of rotating operators

The detailed analysis of squeezing can be performed in a phase-sensitive measurement. For that purpose we define the rotating frame operators as $b(t) = \exp(i\omega_0 t + \theta)a(t)$ and $b^\dagger(t) = \exp(-i\omega_0 t - \theta)a^\dagger(t)$. The rotating SQUID observables are defined analogously as $\phi' = (b(t) + b^\dagger(t))/\sqrt{2}$ and $Q' = i(b^\dagger(t) - b(t))/\sqrt{2}$. The rotating phase factors in $b(t)$ and $b^\dagger(t)$ compensate the natural

rotation of the harmonic creation and annihilation operators. In the new operators the orientation of the squeezing is almost static and determined by the angle θ . The Wigner functions in Fig. 7 appear frozen in time. Only a tiny time-dependent deformations resulting from the driving remains. The noise varies periodically as a function of θ as the orientation of the squeezing is rotated, see Fig. 9. For a finite range of θ the SQUID noise goes below its groundstate value which is a direct evidence of reduction of the quantum fluctuations. For the parameters of Fig. 9, the groundstate noise at zero frequency is approximately 2.5 times higher than the minimum noise corresponding to $\theta = 0$. The noise curves of squeezed states are slightly distorted respect to the origin, which indicates that there is a tiny asymmetry respect to the half axes of the ellipse in Fig. 7. A parametric driving in the presence of a dissipation does not lead to a completely symmetric squeezing.

A phase-sensitive measurements can be realized, for example, with a help of a parametric amplification process.^{3,4} A harmonic modulation of the measurement signal with the frequency ω_0 can be used to measure the rotating spectrum.¹³

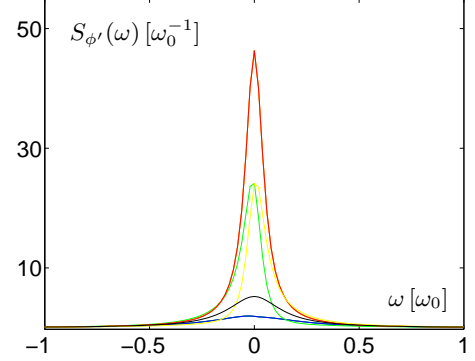


FIG. 9: (Color online) Noise spectrum $S_{\phi'}(\omega)$ of the squeezed state $\kappa = 0.15\omega_0 = 1.25B$ in the rotating operators. The resonance peaks are now moved to the origin. The initial time is chosen so that the minimum noise curve (blue) corresponds to $\theta = 0$. The green, red and yellow curves correspond to the orientations $\theta = \pi/4, \pi/2, 3\pi/4$ respectively. The black curve represents the groundstate noise. The minimum noise curve remain below the groundstate noise, which is an evidence of squeezing.

C. Transmission line output

The TL observables are sum of a free line observables and a retarded SQUID radiation contribution, see Eq. (25). The voltage noise of the TL is of the form $S_V(\omega) = S_V^0 + g^2 S_{\phi'}(\omega)$, where S_V^0 is the vacuum noise of the TL. The coupling constant g depends on the actual material

parameters and can be deduced from Eq. (25):

$$g = \frac{M\omega_0}{L_S} \sqrt{\frac{\hbar Z_0}{2}}, \quad (34)$$

where $Z_0 = \sqrt{L_S/C}$. For the phenomenon to be measurable, the vacuum noise of the TL should not overwhelm the SQUID noise. From Eq. 34 we can estimate the order of magnitude as $g^2 S_{\phi'}(\omega_0) \approx (M/L_S)^2 \hbar \omega_0 Z_0$. At low temperatures the free TL vacuum noise is $S_V^0 = \hbar \omega_0 Z_{\text{TL}}$, where $Z_{\text{TL}} = \sqrt{l/c}$ is the characteristic impedance of the TL. Then the relative effect is of order $g^2 S_{\phi'}(\omega_0)/S_V^0(\omega_0) = (M/L_S)^2 Z_0/Z_{\text{TL}}$. For realistic values $M/L_S = 0.2$, $Z_0 = 500\Omega$ and $Z_{\text{TL}} = 50\Omega$ the fraction becomes $g^2 S_{\phi'}(\omega_0)/S_V^0(\omega_0) = 0.4$, which suggests that the SQUID noise is significant contribution to the TL output radiation in favorable conditions.

VI. CONCLUSIONS

The parametric harmonic driving creates rotating squeezed quantum states in the SQUID ring. If the

environmental damping of the SQUID is negligible the squeezing of uncertainties is exponential for short times. In the presence of a strong damping the magnitude of the squeezing is stationary. The minimum uncertainty in the flux and charge go below the groundstate value periodically. The phenomenon enables a quantum noise engineering which plays an increasingly important role in the quantum measurement theory as well as in the design of practical quantum devices. In principle, squeezed harmonic systems could be used as an ultra sensitive measurement devices of external perturbations coupled to it.^{5,13}

The experimental creation of squeezed quantum states in a SQUID by a parametric driving is feasible with the current experimental methods. We calculated the relevant noise properties of the periodic squeezed state. By introducing a coupling to the transmission line, we analyzed the fully quantum mechanical emission spectrum of the SQUID and discussed briefly the conditions of an experimental verification of the phenomenon.

* Correspondence to teemuo@boojum.hut.fi

- ¹ R. E. Slusher, L. W. Hollberg, B. Yurke, J. C. Mertz and J. F. Valley, Phys. Rev. Lett. **55**, 2409 (1985).
- ² R. Loudon and P. L. Knight, J. Mod. Opt. **34**, 709 (1987)
- ³ B. Yurke *et al.*, Phys. Rev. Lett. **60**, 764 (1988).
- ⁴ B. Yurke *et al.*, Phys. Rev. A **39**, 2519 (1989).
- ⁵ R. Ruskov, K. Schwab and A. N. Korotkov, Phys. Rev. B **71**, 235407-1 (2005).
- ⁶ M. J. Everitt *et al.*, Phys. Rev. A **69**, 043804 (2004).
- ⁷ L. S. Brown and L. J. Carson, Phys. Rev. A **20**, 2486 (1979).
- ⁸ I. Averbukh, B. Sherman, and G. Kurizki, Phys. Rev. A **50**, 5301 (1994).
- ⁹ L. D. Landau and E. M. Lifshitz, *Mechanics* (Pergamon Press, Oxford, 1976).
- ¹⁰ Yu. Makhlin, G. Schön, A. Shnirman, Rev. Mod. Phys. **73**, 357, (1999).
- ¹¹ R. Schoelkopf, A. Clerk, S. Girvin, K. Lehnert, and M. Devoret in *Quantum Noise in Mesoscopic Physics*, ed. by Yu. V. Nazarov, NATO Science Series II Vol. 97 (Kluwer, Dordrecht, 2003);
- ¹² H. J. Carmichael, *Statistical Methods in Quantum Optics 1: Master Equations and Fokker-Planck Equations* (Springer, Berlin, 1999).
- ¹³ V. B. Braginsky and F. Ya. Khalili, *Quantum Measurement* (Cambridge University Press, Cambridge, 1992).